Central European Journal of Energetic Materials
ISSN 1733-7178; e-ISSN 2353-1843

Cent. Eur. J. Energ. Mater., 2016, *13*(4), 957-977; DOI: 10.22211/cejem/65075

Studies of Confined Explosions of Composite Explosives and Layered Charges*)

Lotfi MAIZ*, Waldemar A. TRZCIŃSKI, Mateusz SZALA, Józef PASZULA, Krzysztof KARCZEWSKI

Military University of Technology,
Kaliskiego 2, 00-908 Warsaw, Poland
**E-mail: lotfi.maiz@wat.edu.pl*

Abstract: In the present work, the confined explosions of cylindrical homogeneous and layered charges composed of two different types of macroscopic granular multi-component RDX-based composites were investigated. These composites were obtained by the so-called "wet slurry method". For comparison, charges consisting of simple mixtures instead of the composites, TNT and phlegmatized RDX (RDXph) were also studied. The effect of the following parameters: the structure of the macroscopic granular composite, the type of charge (cylindrical pressed material or layered with an RDXph core), oxygen availability (air or argon atmosphere) and the aluminium particle size, on the quasi-static pressure (QSP) measured inside a 150 dm^3 explosion chamber was determined. Solid post-detonation residues from inside the explosion chamber were also collected and analyzed. A combination of all of these results enabled very important conclusions about aluminium combustion and behaviour during the explosion of composite and layered charges, to be drawn.

Keywords: thermobaric, composite explosives, layered charges, confined explosion, QSP

1 Introduction

Thermobaric explosives (TBXs) and enhanced blast explosives (EBXs) are new types of highly destructive weapons. They are fuel-enriched heterogeneous explosive formulations with high destructive ability and thermal effects. When detonated in a confined space, as well as in environments which promote a rapid

*) Part of this work was presented at the 19th Seminar on New Trends in Research of Energetic Materials, Pardubice, Czech Republic, April 15-17, 2015.

decrease in temperature (free explosions), the metallic fuel incorporated in such charges (usually aluminium) can react with the detonation products or/and oxygen from air, leading to significant additional energy release. In a free explosion, depending on when this energy is generated and how it is used, a charge can be classified as an EBX or a TBX. In fact, during an EBX charge explosion, most of this additional energy is provided from the anaerobic afterburning reactions of the fuel with the detonation products and is used primarily to sustain the blast wave leading to a high specific impulse. However, in a TBX explosion, this energy is largely generated from the later aerobic oxidation reactions of the fuel with oxygen from air, and, as the terminology suggests, this energy is used to increase the temperature and pressure of the explosion [1-3]. When detonated in a confined space, shock wave reflections and mixing of the fuel with the detonation products and air enhance the afterburning reactions, resulting in relatively high values of the quasi-static pressure (QSP) and high destruction ability. In this case, the difference between EBX and TBX charges becomes imperceptible.

Composite EBXs and composite TBXs can be formulated by combining different components such as a high explosive, a metallic fuel, an oxidizer and a binder [3-10]. In layered charges, these components are present in the form of a cylindrical layer surrounding a high explosive core [11-14]. Composite explosives and layered charges formulated from a combination of these components in the form of large macroscopic granules are reported as a separate group of explosives with enhanced combustion effectiveness and improved blast characteristics [2-8].

The explosion of annular charges composed of an RDXph core and a layer consisting of a mixture of ammonium nitrate (AN) and aluminium (Al) powder was studied in paper [13]. From X-ray photographic analysis of the detonating charges it was proved that the detonation phenomenon did not occur in the external layer. However, the measured blast wave characteristics and the light output of the explosion cloud confirmed that initiation of the AN decomposition process and aluminium combustion by the shock wave formed by the expansion of the detonation products of the RDXph core had occurred.

Confined explosion of layered charges composed of an RDXph core and an external layer of aluminium powder or a mixture of ammonium perchlorate (AP) and Al (25/75 or 50/50) was also studied in [14]. Two types of aluminium powder (particle sizes below 44 μm or between 44 μm and 149 μm) were used in the mixtures. Analysis of the results obtained from the chamber led to the conclusion that the application of the outer layer to the RDXph core caused the QSP to be doubled in comparison with the core. A comparison of the measured and theoretical values of the pressure showed that only part of the aluminium

burns during the measurement of overpressure in the chamber (40 ms). In the case of a deficiency of oxygen, AP contributed to the afterburning reactions of aluminium and increased the measured QSP. Post-detonation analysis results revealed that the aluminium powder was almost completely burned after the explosion of the layered charges. However metallic aluminium was still present in the residues after the detonation of charges with Al and AP/Al 25/75 in the external layer in a chamber filled with argon.

In the present paper, cylindrical homogeneous and layered charges composed of two types of granular macroscopic RDX-based composites, obtained by the so called "wet method" [3], were investigated and compared to composite mixtures and common high explosives. For maximization of the generated explosion heat, 30% of two types of aluminium powder and 10% of AP were used [9]. The effects of the macroscopic granular composite structure, the type of charge (cylindrical pressed charge or layered charge with an RDXph core), the aluminium particle size and oxygen availability, on the QSP measured in a confined space were determined. Solid residues from the charge detonations were collected and analyzed.

2 Experimental Approach

2.1 Preparation of the composite materials

Composite explosive formulations consisting of macroscopic energetic granules were investigated. Large macroscopic particles were prepared by using the so called "wet method" [3]. The wet method is a safe, low cost and non-polluting slurry process for obtaining a new class of energetic composite molding granules. Each granule is a complete multi-component energetic macroscopic composite, homogeneous or with granular core-shell structure, comprising a number of crystals of a high explosive, an oxidizer and a metallic fuel, the whole coated and consolidated with a binder. Two kinds of these macroscopic granules were prepared. Each kind of granule was itself a complete multi-component energetic portion containing cyclo-1,3,5-trimethylene-2,4,6-trinitramine (RDX) as a high explosive powder, AP as an oxidizer, Al powder as a metallic fuel, and Viton (a copolymer of vinylidene fluoride and perfluropropylene) as a binder. Crystalline AP with particle size below 0.8 mm and two types of aluminium powder were used. The first type, Al-1, had particles size below 44 μm (325 mesh) and the second, Al-2, had particle sizes between 44 μm and 149 μm (325 mesh to 100 mesh). The first type of granules had a homogeneous structure and was designated by the letter A in Figure 1. The second type was denoted designated B in Figure 1 and

had a core-shell structure. The core comprised a mixture of AP with Al powder consolidated by Viton, with the whole surrounded by an explosive shell.

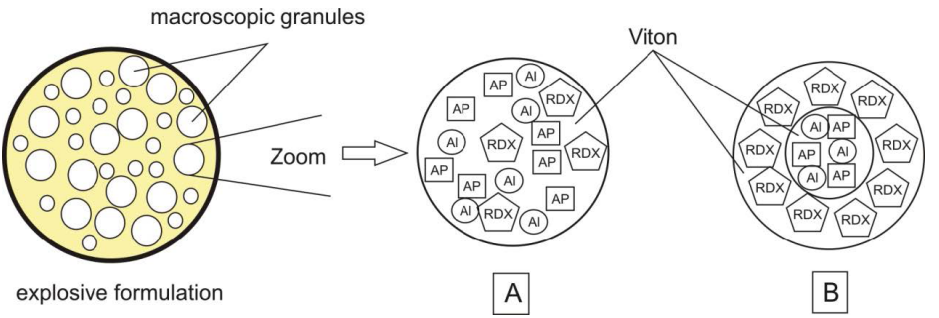

Figure 1. Structures of the macroscopic multi-component granules prepared by the wet method: A − homogeneous configuration, B − core-shell configuration.

During the wet slurry process, Viton as a binder was dissolved in ethyl acetate as the solvent. RDX, AP and aluminium particles were added to this lacquer solution and properly mixed. The macroscopic granules started to form on slow dropwise addition of an anti-solvent. Later, a thermally stable carrier fluid (pharmaceutical paraffin) was added to gradually evaporate both the solvent and the anti-solvent. The wet method needs to be conducted under optimal conditions to obtain homogeneity in granule size, uniformity in coating and high yield. To obtain a core-shell configuration, the wet method was used twice. Firstly the core was prepared from its constituents and set aside to dry. Afterwards, the core and RDX were used as initial ingredients in a saturated binder-solvent solution for the second slurry process (wet method). In this way the core-shell structured macroscopic granules were obtained.

In both A and B configurations, the granules obtained were spherically shaped with a diameter ranging from 1.1 to 1.6 mm. The mass percentage of each ingredient in the composite (granule) is listed in Table 1. Typical photos of the granules are shown in Figures 2 and 3. Complete consolidation of the particles and high adhesion by the binder produced very few voids or cleaved surfaces in the case of granules 21-A. More internal voids were observed in the 21-B granules probably due to the large diameter of the RDX particles. Analysis of the SEM pictures of the 21-B granules and their cross sections showed that granules with a core-shell morphology had been obtained. The AP-Al-Viton core was surrounded by RDX grains consolidated by Viton.

Table 1. Composition of the macroscopic multi-components granules prepared

Structure	Configuration A				Configuration B	
Granule name	11-A	12-A	21-A	22-A	11-B	21-B
Ingredient	Composition [wt.%]					
RDX (crystalline)	50	18.2	50	18.2	50	50
AP	10	18.2	10	18.2	10	10
Al-1	30	54.5	-	-	30	-
Al-2	-	-	30	54.5	-	30
Viton	10	9.1	10	9.1	10	10

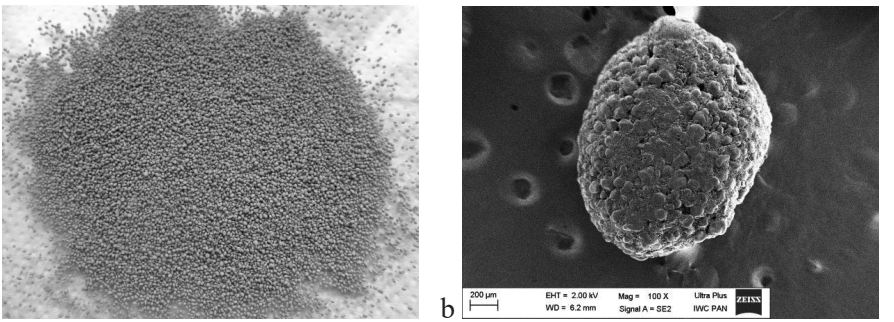

Figure 2. Optical microscope picture (a) and SEM image (b) of composite granules 21-A.

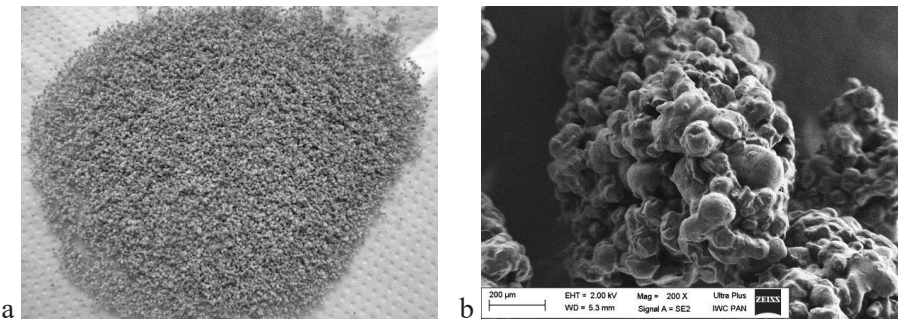

Figure 3. Optical microscope picture (a) and SEM image (b) of composite granules 21-B.

For comparative studies, mixtures of the components were also prepared and designated by C (Table 2). Each component was phegmatized separately using the wet method. The amount of binder (Viton) for each component was chosen to be proportional to each component percent content so that the final mixture had the same mass composition as formulations A from Table 1.

Table 2. Composition of the mixtures

Mixture name	11-C	12-C	21-C	22-C
Ingredient	Composition [wt.%]			
RDX (crystalline)	50	18.2	50	18.2
AP	10	18.2	10	18.2
Al-1	30	54.5	-	-
Al-2	-	-	30	54.5
Viton	10	9.1	10	9.1

2.2 Characteristics of the charges

To investigate the influence of charge type, aluminium particle size and the configuration of the composites (structures A, B or mixture C) on the blast parameters in a confined explosion, two kinds (layered and homogeneous) of cylindrical charges containing the different composites were prepared. All charges had the same mass of 43 g and the same total composition. The heterogeneous charges prepared for this work are defined in Tables 3 and 4. All of the composites and mixtures containing 50% of RDX in configurations A, B and C, were pressed using a hydraulic press into 25 mm diameter cylindrical pellets. This type of charge is named hereafter as homogeneous charges TBX-*x*, where symbol *x* is the name of the composite or the name of the mixture – Table 3. A cross section of a homogeneous charge is shown in Figure 4. The second kind of charge is described in Table 4 and Figure 5. The cylindrical layered charge consisted of a core and an external layer. The core was constructed from two cylindrical pellets of RDX phlegmatized by 6 wt.% of wax (RDXph). The total mass of the core was 18.3 g, its diameter and density were 16 mm and 1.69 g/cm^3, respectively. This type of charge is named hereafter as layered charges TBX-*x*', where symbol *x*' is the name of the composite or the name of the mixture – Table 4. The external layer had a mass of 24.7 g of a given composite or mixture. The external cylinder was a paper tube having a thickness of about 2 mm and an internal diameter of 30 mm. The mass of the core and the external layer were selected in such a way that the total mass of the charges and the percent of each constituent were identical to the homogeneous charges. For comparison, tests were also performed with 43 g of pressed TNT (cylindrical trinitrotoluene charges of 25 mm in diameter with a density of about 1.53 g/cm^3) and 43 g or 18.3 g (mass of the core) of RDXph (cylindrical charges with density of 1.69 g/cm^3 and a diameter of 25 mm for the larger charges; the smaller RDXph cores were exactly similar to the cores used in the layered charges and are named RDXph core).

Table 3. Characteristics of the cylindrical homogeneous charges

Symbol	TBX-11-A	TBX-21-A	TBX-11-B	TBX-21-B	TBX-11-C	TBX-21-C
Mass [g]	43	43	43	43	43	43
Density [g/cm^3]	1.87	1.90	1.73	1.74	1.76	1.79
Diameter [mm]	25	25	25	25	25	25

Table 4. Characteristics of the cylindrical layered charges

Symbol	TBX-12-A	TBX-22-A	TBX-12-C	TBX-22-C
Mass [g]	18.3/24.7 (core/layer)	18.3/24.7	18.3/24.7	18.3/24.7
Density [g/cm^3]	1.69/1.23 (core/layer)	1.69/1.23	1.69/1.21	1.69/1.22
Diameter [mm]	16/30 (core/layer)	16/30	16/30	16/30

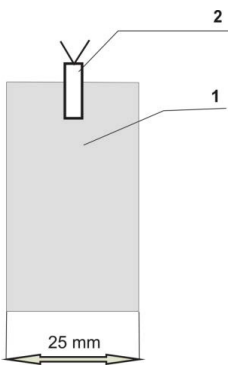

Figure 4. Schematic of the investigated homogeneous charges: 1 – composite or mixture, 2 – detonator.

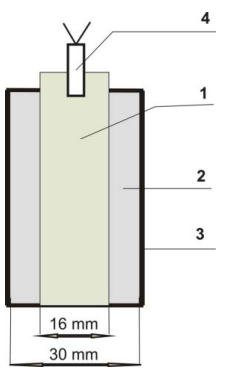

Figure 5. Schematic of the investigated layered charges: 1 – RDXph, 2 – composite or mixture, 3 – paper tube, 4 – detonator.

2.2 Confined explosion procedure

Quasi-static pressure (QSP) tests for all of the charges were performed in a closed explosion chamber of volume 0.15 m^3. The dimensions of the explosion chamber are shown in Figure 6. A charge was hung in the center of the chamber and a standard fuse was used to initiate detonation. A standard electrical detonator was enough to detonate all of the layered charges and the TBX-A charges; however, a booster consisting of 5 g of pressed RDXph was necessary to initiate the detonation of the TBX-B charges and the homogeneous TBX-C charges. A mass of 1.3 g of PETN (pentaerythritol tetranitrate) was assumed as an energetic equivalent of the detonator. Primary tests were carried in an air atmosphere under normal pressure of about 0.1 MPa and at ambient temperature. Then four type of charges were selected for further tests in argon under the same conditions. In this case, in order to expel air from the chamber, the latter was filled with argon up to a pressure of 0.25 MPa and then emptied three times. After filling for the final time to a pressure of 0.1 MPa the chamber was ready for the tests under an argon atmosphere. In both atmospheres, air and argon, at least three tests were performed for each charge investigated. Signals of the overpressure from two piezoelectric gauges (PCB Piezotronics, models 102A and 102B) located at the chamber wall were recorded by a digital storage scope. The surface of the pressure sensors was covered by plastic material in such a way as to protect them from jets and hot explosion products. After each test, the residues were collected for analysis and the chamber was cleaned for the following tests.

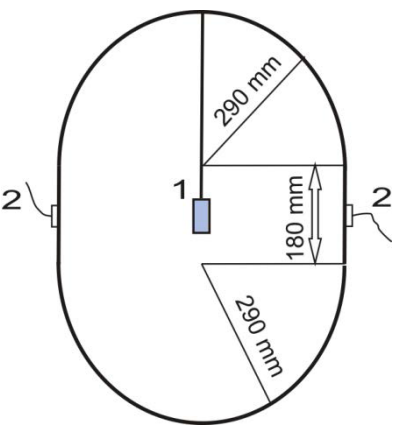

Figure 6. Schematic diagram of the 0.15 m^3 explosion chamber (side view): 1 – explosive charge, 2 – pressure gauges.

3 Results and Discussion

3.1 Quasi-static pressure results in air

The overpressure history records have an oscillating nature caused by shock reverberations at the chamber wall, shock reverberations inside the chamber, turbulence of the hot explosion products and vibrations of the measuring system. The amplitude of these oscillations decreased with time. Equation 1 was used for the overpressure history approximation (Δp).

$$\Delta p = ce^{-dt} + a(1 - e^{-bt}) \tag{1}$$

where a, b, c and d are constants, t is time. The first term in Equation 1 describes the small decrease observed in the average overpressure history during the recording time (40 μs). The second term indicates the growth in this average overpressure which was caused by combustion of the aluminium particles inside the explosion chamber. Typical overpressure histories recorded for some charges, as well as their approximations, are shown in Figure 7. Function 1 reaches a maximum value Δp_{max} for a time t_{max} (Equation 2). If t_{max} is outside the investigated time interval Δp_{max} is equal to the constant c corresponding to $t = 0$ s.

$$t_{max} = \ln\left(\frac{ab}{cd}\right)\frac{1}{b-d} \tag{2}$$

Thermochemical calculations were also performed to estimate the final overpressure in the chamber. The CHEETAH code with modified library was used for this purpose with the set of values of the BKW parameters: $\alpha = 0.50$, $\beta = 0.40$, $\kappa = 10.86$ and $\Theta = 5441$ K [16]. The overpressure Δp_{cal} was calculated for a constant volume state determined for an explosive charge and air enclosed in the chamber. Thermochemical equilibrium was assumed in these calculations. For aluminized charges, an overpressure (Δp_{inr}) was also calculated with the assumption of aluminum chemical inertness (no reaction between the aluminum particles and gases inside the chamber). The fuse explosive (PETN) was included in the calculations. Values of Δp_{max} (QSP) with standard deviations determined on the basis of at least six overpressure histories recorded in the chamber filled with air and Δp_{cal} obtained from thermochemical calculations are summarized in Table 5 for all of the charges tested.

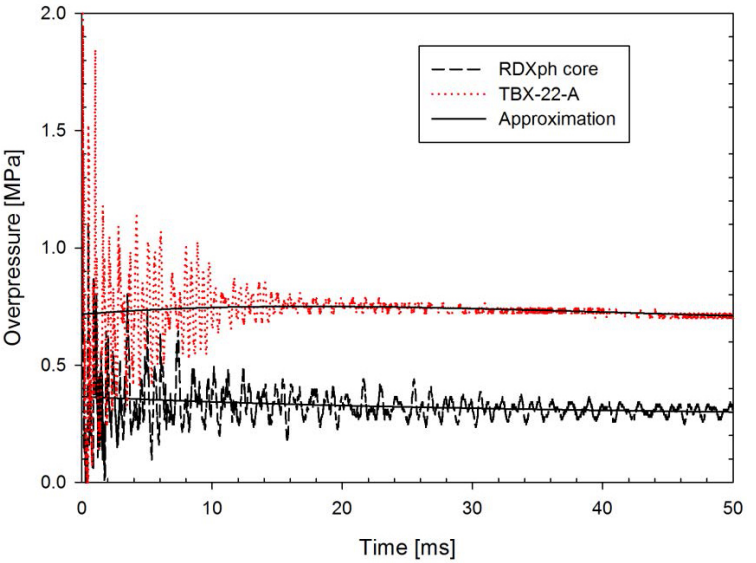

Figure 7. Typical overpressure histories recorded for RDXph core and TBX-22-A charges in air.

An analysis of the data in Table 5 shows that all values of Δp_{max} are lower than the calculated Δp_{cal} for all charges. In fact, theoretical calculations were run under the assumption of thermochemical equilibrium of the reactive mixture, but this assumption does not describe exactly the phenomena inside the explosion chamber, since mixing of component as well as their thermal equilibrium are not perfect, especially during the first 50 ms. The QSP values of aluminized charges were lower than the theoretical ones if it is assumed that all aluminium reacts, but significantly higher than those calculated under the assumption of thermochemical equilibrium and non-reactivity of aluminium particles. Moreover, all maximum overpressures measured for the aluminized charges are superior to those of TNT or RDXph. This indicates that aluminium from the compositions reacts with the detonation products and/or air in the explosion chamber resulting in additional heat which increases the temperature and pressure of the gaseous mixture. The overpressures obtained for the charges with cylindrical fuel-rich layer at least doubled the value of QSP determined for the RDXph core only.

The aluminium powder size, type of charge and composite structures (A, B or mixtures C) all affect the ratio of the measured maximum overpressure and the calculated average pressure $\Delta p_{max}/\Delta p_{cal}$. In fact, homogeneous charges with small aluminium particle size have a higher ratio than homogeneous charges with larger aluminium particles and the inverse tendency is observed in the case

of layered charges. This means that the kinetics, and probably the mechanism, of the aluminium reaction is different in the case of a confined homogeneous charge explosion and a confined layered charge explosion due to the fact that the processes of detonation of homogeneous charges and layered charges in the explosion chamber run in different ways. Better conditions (a specific area, an increase in the temperature inside the particles) occur for the combustion of fine aluminium in the case of homogeneous charge detonation than for coarse aluminium. However, the conditions are more favorable for the combustion of larger aluminium particles when a layered charge is detonated in the chamber and they move quickly into air. When it comes to comparison between homogeneous and layered charges, obviously the homogeneous charges are better than the layered ones for small aluminium particles but worse for larger aluminium particles. These conclusions are valid for the A composites and also the C mixtures.

Table 5. Values of the maximum overpressure measured in air and calculated by the CHEETAH code

Charge	Δp_{max} [MPa]	Δp_{cal} [MPa]	$\Delta p_{max}/\Delta p_{cal}$ [%]	$\Delta p_{max}/\Delta p_{RDX\ core}$ [%]	Δp_{inr} [MPa]
TBX-11-A	0.79±0.02	0.98	80.61	-	0.50
TBX-12-A	0.77±0.03	0.98	78.57	2.08	0.50
TBX-21-A	0.76±0.04	0.98	77.55	-	0.50
TBX-22-A	0.79±0.08	0.98	80.61	2.14	0.50
TBX-11-B	0.82±0.06	1.04	78.85	-	0.56
TBX-21-B	0.78±0.03	1.04	75.00	-	0.56
TBX-11-C	0.80±0.03	1.04	76.92	-	0.56
TBX-12-C	0.74±0.02	0.98	75.51	2.00	0.50
TBX-21-C	0.78±0.06	1.04	75.00	-	0.56
TBX-22-C	0.80±0.07	0.98	81.63	2.16	0.50
TNT	0.75±0.06	1.03	72.82	-	-
RDXph	0.70±0.01	0.92	76.09	-	-
RDXph (core)	0.37±0.03	0.47	78.72	1	-

Concerning the composite granular structure effect, it was observed that the overpressure ratio is superior for charges containing the A composite compared to the B composite and to the C mixture for both homogeneous and layered charges. This order is also preserved in the case of smaller aluminium particles (except for composition TBX-22-C) or larger particles. More intimate contact and homogeneous distribution of the ingredients is provided by the macroscopic

configuration A compared to B and to the mixture C. Contrary to our expectations, the outer RDX-Viton shell surrounding the Al-AP core in the macro fragments B did not have an enhancing effect on aluminium combustion; probably not enough heat was being transferred to the core for aluminium initiation because of the distance between RDX in the shell and Al in the core, or the quantity of AP is not enough to provide the oxygen. The first explanation could be more likely.

3.2 Quasi-static pressure results in argon

To investigate the detonation and explosion of aluminized charges in the absence of oxygen (air), further tests were carried out in the chamber filled with argon. These tests allowed us to determinate the contribution of the anaerobic reactions of aluminium particles in the overpressure history inside the explosion chamber by comparing them with tests in air. The only chemical afterburning reactions are between aluminium and the hot gaseous detonation products. The compositions TBX-A were selected for these trials. In fact, the composite granules A showed the best properties during preliminary research [3] (SEM observations, TG/DTA analysis, friction and impact sensitivity tests) and the best ratios of $\Delta p_{max}/\Delta p_{cal}$ were determined for the chamber filled with air for both homogeneous and layered charges.

Equation 1 was used to determine the maximum overpressure inside the chamber. Theoretical calculations were performed with the assumption of reaction of aluminium with the hot detonation gases, and for inert aluminium. The average QSP or Δp_{max} values for all TBX-A charges, and TNT and RDXph charges, measured in argon are summarized in Table 6. The QSP for TNT charges was obtained from 12 recordings of overpressure histories (6 shots). The parameter of $\Delta p_{O\text{-}Ar}$ is the difference in values of the maximum overpressure determined experimentally in air and argon.

Table 6. Values of the maximum overpressure measured in argon and calculated by the CHEETAH code with an extended library for TBX-A, TNT and RDXph charges

Charge	Δp_{max} [MPa]	Δp_{cal} [MPa]	$\Delta p_{max}/\Delta p_{cal}$ [%]	Δp_{inr} [MPa]	$\Delta p_{O\text{-}Ar}$ [MPa]
TBX-11-A	0.66±0.06	0.96	68.75	0.47	0.13
TBX-12-A	0.60±0.02	0.96	62.50	0.47	0.17
TBX-21-A	0.69±0.04	0.96	71.88	0.47	0.07
TBX-22-A	0.61±0.02	0.96	63.54	0.47	0.18
TNT	0.52±0.05	0.47	110.64	-	0.23
RDXph	0.52±0.05	0.70	74.29	-	0.18

Concerning aluminized charges in argon, the values of the maximum average overpressure are smaller than those in air because of the absence of oxygen. This means that aerobic reactions of aluminium take place in the chamber filled with air and they lead to the release of additional heat and increase of the overpressure. However, the QSP values in the chamber filled with argon are higher than Δp_{inr}, which means that aluminium also takes part in anaerobic afterburning reactions with the hot detonation products.

It is clear that in the absence of oxygen from air, the homogeneous charges have higher values of QSP than the layered ones. This simply shows that pressed cylindrical charges (homogeneous) promote the anaerobic reactions of aluminium particles with the detonation products, probably because the mixing of aluminium and the detonation products is better than for the layered charges. Moreover, $\Delta p_{O\text{-}Ar}$ for the homogeneous charges are lower than $\Delta p_{O\text{-}Ar}$ for the layered charges, especially for TBX-21-A. This indicates that unlike the layered charges, a large part of the aluminium in the homogeneous charges can react aerobically. It demonstrates that the homogeneous charges can be considered as enhanced blast explosives (EBXs). Surprisingly, the QSP recorded for TBX-21-A is superior to that recorded for TBX-11-A, and consequently, coarse aluminium is more able to react with the detonation products in the absence of oxygen. However, the difference between these values is much smaller than the standard deviation, and, in fact, this relation may be reversed.

In the layered charges, $\Delta p_{O\text{-}Ar}$ is high, which means that unlike the homogeneous charges, the explosion of the layered charges promotes aerobic afterburning reactions of aluminium even in closed spaces, since they are thermobaric.

The value of Δp_{cal} determined experimentally for TNT charges under argon is similar to that of RDXph. Moreover, it is unexpectedly higher than the theoretical one. The following explanation is proposed. The TNT detonation process produces high pressure and temperature of products composed of species including C, CO, H_2, a variety of hydrocarbons (TNT has an oxygen balance of −74%) and also CO_2 and H_2O. Depending on the conditions, these detonation products have the potential to reaction further. When all the required conditions for reaction with oxygen exist (enough oxygen, good mixing between the detonation products and oxygen from air and a temperature higher than the ignition temperature of the reactions), CO and H_2 (and other species) react with oxygen to form CO_2 and H_2O. During this afterburning process important additional heat is liberated, and this heat can be used to increase the pressure inside the chamber. In the absence of oxygen, and at high temperature and relatively low pressure, the creation of H_2 and CO species is promoted during the

endothermic reactions [17-21], heat is absorbed and, consequently, the pressure inside the chamber is decreased.

As was explained earlier, an ideal equilibrium of the species present after explosion in the chamber is assumed in the thermochemical code CHEETAH. In the absence of oxygen and under conditions of high temperature and low pressure, secondary reactions leading to CO and H_2 formation, and CO_2 and H_2O elimination, are promoted; consequently the heat generated by the TNT explosion in the chamber is lower than its heat of detonation. However, in reality, argon acts as a diluent (mixing, turbulence, diffusion) for the detonation products and as a barrier between the chemical species present in the chamber. In this case, no extra-reactions occur after the shock reverberation from the wall. Consequently, the processes of CO_2 and H_2O elimination and CO and H_2 creation stop. This leads to smaller heat decreases and higher explosion energy than in the ideal case. Therefore, the measured overpressure inside the chamber is higher than the calculated one.

3.3 Analysis of the post-explosion solid products

Solid products from the explosions of the TBX-A charges in air and in argon atmospheres were collected, washed with distilled water, filtered, and dried for 24 h at 100 °C. SEM, DTA/TG and XRD analyses were made to determinate their morphology, and their chemical and phase compositions. From visual observations, it appeared clearly that the colour and consistency of the residues from the chamber filled with air were different from when argon was used. In the case of detonations in argon, the residues were in the form of very fine black powders, probably because of the presence of carbon soot. When air was in the chamber, the residue particles were larger and white metallic colour was visible.

3.3.1 SEM analysis

Scanning electron microscopy (SEM) (Quanta 3D FEG Dual Beam, operating at 20 kV) was used for microstructural observation of the residues. For a specific filler gas (air or argon), the SEM images of the analyzed residues were similar, irrespective of the type of charge or the aluminium particle size. Only the atmosphere inside the chamber affected the SEM images of the collected residues. Typical SEM images of the residues are shown in Figures 8 and 9.

For a better interpretation of the SEM images, it should be noted that the final theoretical explosion temperature in the chamber filled with air was 2882 K if the aluminium was assumed to be reactive in the calculations, and 1522 K for inert aluminium. Therefore, the aluminium oxide formed after the aluminium reaction could reach a liquid state (melting point of aluminium oxide is about 2345 K).

However, the heat liberated during the explosion in air was undoubtedly enough to increase the temperature above the melting point of aluminium (933.47 K). In the case of argon in the chamber, the final theoretical explosion temperature was 2278 K for reactive aluminium and 947 K for inert aluminium.

Two types of spherical particles were observed in all samples collected from charges detonated in air (Figure 8a). Spherical solidified droplets having a diameter of tens of micrometers were the first type. Their number was small and were characterized by a metallic colour in the SEM images. These are probably non-oxidized aluminium droplets. The second type of particles predominated, these were regular shaped spheres with a diameter lower than 1 mm and had a white colour in the SEM images. These submicron particles were composed of aluminium oxide, formed by oxidation of aluminium in tiny liquid droplets, which had become nearly spherical due to surface tension. This means that aluminium must be in the form of submicron liquid droplets to react and create aluminium oxide during the explosion. Part of the aluminium in the form of melt droplets which was not oxidized, gathered and condensed to create the first type of metallic microparticles, and the other part formed a matrix which welded the aluminium oxide particles together to form large agglomerates of granules after condensation (Figure 8b).

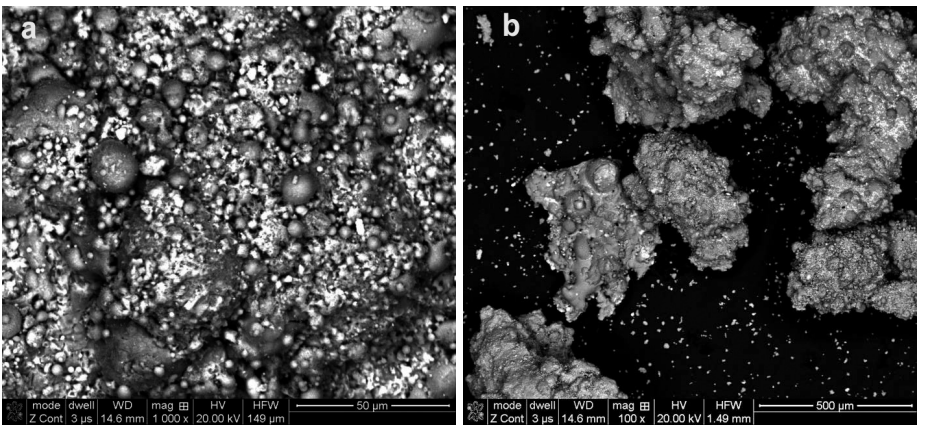

Figure 8. Typical SEM images of the residue of TBX-11-A detonated in air.

Samples collected from charges detonated in argon contained mostly irregularly shaped particles of a few microns in diameter, probably mixtures of partially oxidized aluminium (oxygen from AP and detonation products) and carbon soot (Figure 9a). Unlike the samples collected from explosions in air, these particles were rarely agglomerated in the form of macroscopic granules

(no welding) (Figure 9b). This indicates that just a small amount of aluminium was in the liquid state during the explosion. As in the case of detonations in air, shock waves shattered the initial macroscopic composite granules, but unlike detonations in air, only a small part of the aluminium was melted by the heat released by the detonation. A very small amount of aluminium reacted with the detonation products and oxygen from AP, but after mixing with argon, the combustion of the aluminium was stopped. Another important observation was that for both sizes of aluminium particles used in the charges (Al-1 and Al-2), the SEM pictures of the solid residues were very similar with the same size of aluminum spheres (solidified droplets). This means that aluminium of any particle size is shattered to microparticles by the shock waves. Actually, the particle size is not important but the ratio of pure aluminium to the passivating alumina layer on the surface of the particles is important.

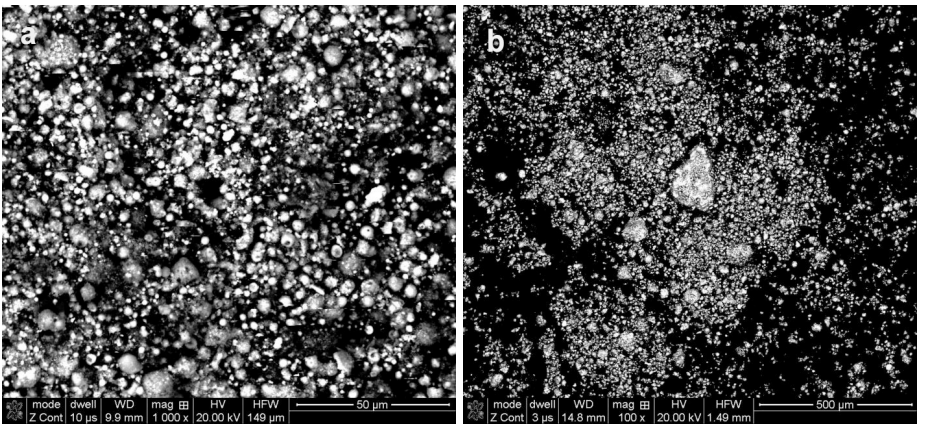

Figure 9. Typical SEM images of the residue of TBX-11-A detonated in argon.

3.3.2 TG/DTA analysis

TG/DTA measurements were performed using a Labsys TG/DTA-DSC apparatus. Samples were placed in open alumina crucibles with Al_2O_3 in the reference pan. All thermograms were recorded at 10 K/min heating rate in a synthetic air atmosphere (N_2/O_2 79/21 by volume). The gas flow rate was 50 cm^3/min. Thermograms of the residues of charges detonated in air are presented in Figure 10. The behaviour of the samples can be divided into three phenomenological stages. In the first stage, corresponding to temperatures from 30 °C to 150 °C, the sample mass diminished between 0.3% and 2% (the highest was observed for TBX-12-A). According to the DTA curves, this is an endothermic process caused by the evaporation of water and absorbed gases.

The second stage started from about 200 °C. Except for the sample from the TBX-12-A explosion, the thermograms showed slow mass loses and wide exothermic peaks, corresponding to the oxidation of carbonaceous detonation products. However the slow mass reduction indicated that the residues contained mainly heat- and oxygen-resistant ingredients, probably Al_2O_3. At approximately 655 °C, small endothermic peaks (melting points of aluminium) indicated that part of the aluminium remained in the explosion products. The last stage started at about 850-865 °C. An increase in the sample mass was recorded as well as an exothermic peak, which indicated the oxidation of aluminium. Melting of aluminium starts at 655 °C, however, its oxidation does not commence until 850 °C, probably because it is covered by a thick layer of aluminium oxide. Therefore, metallic aluminium remained inside the small submicron spheres which are observed in the SEM images.

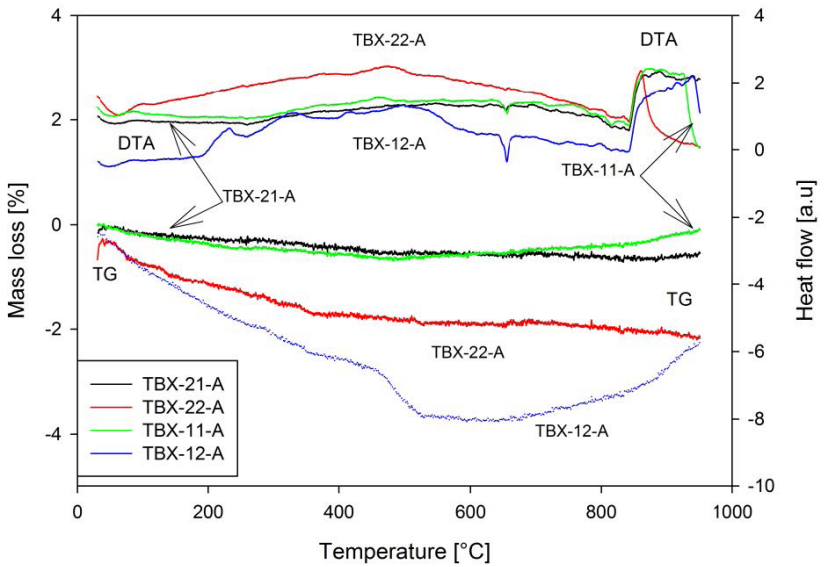

Figure 10. TG/DTA thermograms of residues collected from charges detonated in air.

After detonation in an argon atmosphere, the residues contained more metallic aluminium and carboneous material; in fact, the mass reduction was about 3% to 9% during heating below 600 °C (Figure 11). A sharp endothermic peak in the DTA curves indicated that the unburned aluminium started to melt at about 655 °C. However, unlike the samples from detonation in air, aluminium started to oxidize directly after melting and an increase in the mass on the TG

curves was observed. The aluminium oxidation was recorded at the same temperature or sometimes lower than the melting point of aluminium, probably because the particles were not covered by a thick alumina layer.

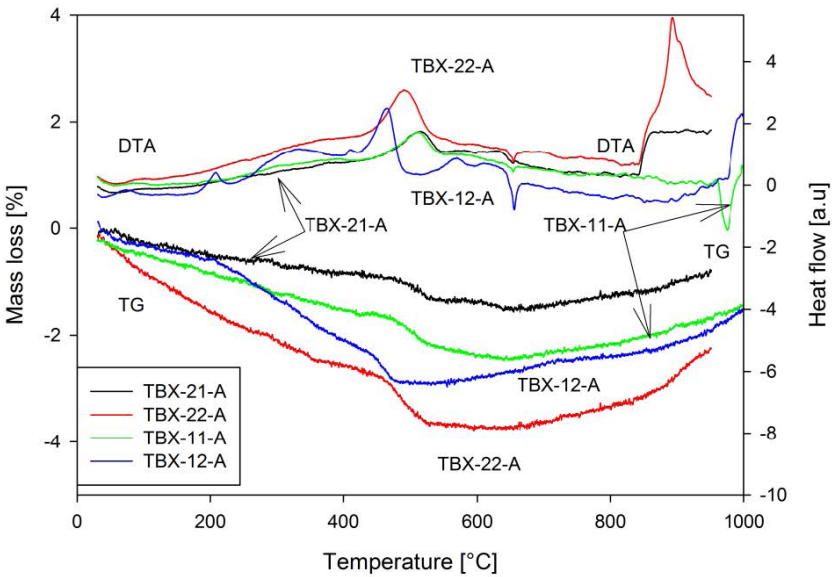

Figure 11. TG/DTA thermograms of residues collected from charges detonated in argon.

3.3.3 XRD analysis

The composition and crystal structure of the solid residues were characterized using X-ray diffraction (XRD) (diffractometer Rigaku Ultima IV with Co $K\alpha_1$ radiation of 1.79 Å). The scan range angle was from $2\Theta = 20 - 140°$ in increments of 0.02°. For the analysis of the spectra obtained, the ICDD database PDF4 of standard diffraction patterns was used.

Chemical species and phases identified in the solid residues from charges detonated in air are shown in Table 7. The alumina found in all residues had rhombohedral crystal structure and a cubic structure in one case (04-015-6810). Iron and iron oxide were also present because the explosion chamber was made of steel. Crystallites of aluminium were found only in the detonation of charge TBX-21-A, probably because in the other samples the aluminium was covered by a thick layer of aluminium oxide which the X-ray beam cannot penetrate (the presence of aluminium in the residues from detonations in air was proved by the thermal analysis).

The results of the XRD analyses for the residues from detonations in argon are presented in Table 8. Aluminium was present in all samples. As was explained before, the reaction of this is stopped by the argon atmosphere during the explosion. Aluminium nitride was also found. Rhombohedral corundum aluminium oxide was the main phase matched in the residues from the chamber filled with argon.

Table 7. Matched phases in the solid residues recovered from the chamber filled with air

Charge	Aluminium	Aluminium oxide	Aluminium nitride	Iron	Iron oxide
TBX-11-A	no	04-005-4505 01-071-1683	no	04-016-6640	01-080-5414
TBX-12-A	no	01-075-1862	no	no	04-015-9906
TBX-21-A	04-014-0129	04-005-4505 04-015-6810	no	04-016-6640	01-080-5414
TBX-22-A	no	04-005-4505	no	04-016-6640	01-080-5414

Table 8. Matched phases in the solid residues recovered from the chamber filled with argon

Charge	Aluminium	Aluminium oxide	Aluminium nitride	Iron	Iron oxide
TBX-11-A	04-013-5553	04-015-8608	01-088-2250	04-016-6640	01-080-5414
TBX-12-A	04-013-5553	01-075-1862	04-013-4807	no	04-015-9906
TBX-21-A	04-014-0129	04-005-4505	04-004-4544	04-016-6640	01-080-5414
TBX-22-A	04-014-0129	01-089-7715	01-088-2250	04-006-4261	04-015-9906

4 Conclusions

Analysis of the results obtained in this work enabled us to draw the following conclusions:

1. Quasistatic pressures measured in the chamber filled with air for aluminized charges are lower than the theoretical averaged pressures calculated for chemically active aluminium but significantly higher than those calculated under the assumption of inert aluminium.
2. Type of charge and composite structures affect the values of the quasistatic pressures inside the confined explosion chamber and the effect of aluminum powder size is ambiguous.

3. Homogeneous charges with fine aluminium have higher values of the pressure ratio than homogeneous charges with coarse aluminium and an inverse tendency is observed in the case of layered charges. This means that homogeneous charges are better than layered ones for small aluminium particles but worse for larger aluminium particles.
4. In the layered charges, the cylindrical fuel-rich layer at least doubles the value of the overpressure in comparison with the RDXph core.
5. Aerobic reactions of aluminium occur in the chamber filled with air and lead to liberation of the main part of the additional heat.
6. The explosion of layered charges in an argon atmosphere promotes aerobic afterburning reactions of aluminium.
7. From TG/DTA and XRD analyses of the chamber residues it follows that aluminium is not completely burned after the explosion of the composite and layered charges, either in air or argon.

References

[1] Peuker J.M., Krier H., Glumac N., Particle Size and Gas Environment Effects on Blast and Overpressure Enhancement in Aluminized Explosives, *Proc. Combust. Inst*., **2013**, *34*, 2205-2212.
[2] Trzciński W.A., Maiz L., Thermobaric and Enhanced Blast Explosives – Properties and Testing Methods (Review), *Propellants Explos. Pyrotech.*, **2015**, *40*(4), 632-644.
[3] Maiz L., Trzciński W.A., Szala M., Preparation and Testing of Thermobaric Composites, *New Trends Res. Energ. Mater., Proc. Semin., 18th*, Pardubice, Czech Republic, **2015**, 705-715.
[4] Guirguis R.H., *Reactively Induced Fragmenting Explosives*, Patent US 6 846 372 B1, **2005**.
[5] Newman K.E., Riffe V., Jones S.L., Lowell M.D., *Thermobaric Explosives and Compositions, and Articles of Manufacture and Methods Regarding the Same*, Patent US 7 754 036 B1, **2010**.
[6] Baker J.J., *Thermobaric Explosives, Articles of Manufacture, and Methods Comprising the Same*, Patent US 7 807 000 B1, **2010**.
[7] Sheridan E.W., Hugus G.D., Brooks G.W., *Enhanced Blast Explosives*, Patent US 7 998 290 B2, **2011**.
[8] Nicolich S.M., Capellos C., BalasW.A., Akester J.D., Hatch R.L., *High-blast Explosive Compositions Containing Particulate Metal*, Patent US 8 168 016 B1, **2012**.
[9] Trzciński W.A., Cudziło S., Paszula J., Studies of Free Field and Confined Explosions of Aluminium Enriched RDX Compositions, *Propellants Explos.*

Pyrotech., **2007**, *32*(6), 502.
[10] Trzciński W.A., Cudziło S., Paszula J., Callaway J., Study of the Effect of Additive Particle Size On Non-ideal Explosive Performance, *Propellants Explos. Pyrotech*., **2008**, *33*(3), 227.
[11] Chan M.L., Meyers G.W., *Advanced Thermobaric Explosive Compositions*, Patent US 6 955 732 B1, **2005**.
[12] Chan M.L., Bui D.T., Meyers G., Turner A., *Castable Thermobaric Explosive Formulations*, Patent US 6 969 434 B1, **2005**.
[13] Trzciński W.A., Barcz K., Investigation of Blast Wave Characteristics for Layered Thermobaric Charges, *Shock Waves*, **2012**, *22*(2), 119.
[14] Trzciński W.A., Barcz K., Paszula J., Cudziło S., Investigation of Blast Performance and Solid Residues for Layered Thermobaric Charges, *Propellants Explos. Pyrotech*., **2014**, *39*(1), 40.
[15] Fried E., *CHEETAH 1.39 – User's Manual*, Lawrence Livermore National Laboratory,1**996**.
[16] Fried L.E., Souers P.C., BKWC: an Empirical BKW Parametrization Based on Cylinder Test Data, *Propellants Explos. Pyrotech.*, **1996**, *21*(4), 215.
[17] Ornellas D.L., The Heat and Products of Detonation of Cyclotetramethyletetranitamine, 2,4,6-Trinitrotoluene, Nitromethane, and Bis[2,2-dinitro-2-fluoroethyl]formal, *J. Phys. Chem*., **1968**, *72*, 2390.
[18] Ornellas D.L., *Calorimetric Determination of the Heat and Products of Detonation for Explosives*, Report UCRL 52821, Lawrence Livermore National Laboratory, **1982**.
[19] Wolański P., Gut Z., Trzciński W.A., Szymańczyk L., Paszula J., Visualization of Turbulent Combustion of TNT Detonation Products in a Steel Vessel, *Shock Waves*, **2000**, *10*(2), 127-136.
[20] Trzciński W.A., Paszula J., Wolański P., Thermodynamic Analysis of Afterburning of Detonation Products in Confined Explosions, *J. Energ. Mater*., **2002**, *20*(3), 195.
[21] Kiciński W., Trzciński W.A., Calorimetry Studies of Explosion Heat of Non-ideal Explosives, *J. Therm. Anal. Calorim*., **2009**, *96*(2), 623.